

OMEGA SYNCHRONIZATION: CURRENT OPERATIONS AND FUTURE PLANS

Howard J. Santamore
U.S. Coast Guard, Washington, D.C.

Roger N. Schane, Stephen F. Donnelly,
The Analytic Sciences Corporation, Reading, Massachusetts

ABSTRACT

Modern estimation techniques are applied to the problem of synchronizing OMEGA VLF signal transmissions from geographically-remote transmitter stations. Each OMEGA transmitter is controlled by its own bank of four cesium beam atomic frequency standards. A synchronization computer program SYNC2* combines models of cesium clock error dynamics with OMEGA phase timing measurements to estimate and control inter-transmitter synchronization offsets (both phase and phase rate) to an accuracy on the order of 1 μ sec rms.

Auxiliary algorithms perform OMEGA phase measurement preprocessing, including: compensation for propagation anomalies, reciprocal path phase differencing, automatic outlier rejection, dynamic measurement-quality weighting, and time-correlation modeling. Alternative timing measurements (including: satellite/TV, Loran-C, and portable clock) are utilized, as available, to synchronize the entire transmitter system to Coordinated Universal Time (UTC) as maintained by the United States Naval Observatory (USNO).

Future plans for OMEGA synchronization include: increased use of non-VLF propagation models, and active participation by the Japanese Maritime Safety Agency (JMSA) in Program SYNC2 operation.

*This program was developed at The Analytic Sciences Corporation (TASC) for the U.S. Coast Guard OMEGA Navigation System Operations Detail (ONSOD) under Contract No. DOT-CG-23735-A.

INTRODUCTION

OMEGA is a long-range, all-weather, radio navigation system consisting of eight transmitter stations, strategically located around the world. Each transmitter generates continuous-wave, phase-locked, very-low-frequency (VLF) signals between 10.2 and 13.6 kHz. OMEGA provides a unique combination of worldwide navigation capability and bounded position errors, typically on the order of 1 to 2 nm rms.

VLF signals propagate in a natural waveguide between the earth's surface and the ionosphere, and maintain a nearly linear relationship between signal phase and distance from each transmitter. Phase difference measurements from pairs of transmitters define earth-referenced hyperbolic lines-of-position (LOPs) which are used for position determination. Certain geophysical factors (e.g., variations in solar illumination, geomagnetic field, and ground conductivity) tend to distort this linear phase/distance relationship and, thus, limit position accuracy. Models have been developed [1] to partially compensate for VLF phase propagation variations, and tables of Predicted Propagation Corrections (PPCs) have been computed [2] and published [3].

Use of phase differences for OMEGA navigation requires precise phase synchronization of signals from all OMEGA transmitters. (A six microsecond synchronization offset between two transmitters can result in a 1 nm position error.) The phase of each OMEGA transmitter is controlled by its own online cesium clock (and several backup clocks). A cesium clock determines precise time intervals by counting oscillation periods of a cesium-beam atomic frequency standard. For two clocks to be perfectly synchronized, their frequency standards must match perfectly in both phase and frequency. In general, there are small uncontrollable differences (on the order of 0.03 to 0.3 usec/day) in the cesium frequencies of different online clocks. These relative frequency offsets result in inter-transmitter phase (or timing) offsets that can increase with time, if uncorrected.

To prevent uncontrolled time offset growth in the OMEGA system, internal synchronization is accomplished by periodically adjusting the epoch (i.e., time or phase) of each OMEGA transmitter to the average epoch of all transmitters (Mean OMEGA System Time). External synchronization, which is not necessary for navigation, but is for time dissemination, is established by maintaining Mean OMEGA System Time at a known constant offset from UTC as maintained by the U.S. Naval Observatory (USNO).

Transmitter phase (epoch) adjustments are computed weekly by processing both internal and external timing measurements. Internal measurements indicate the relative timing offsets between pairs of OMEGA transmitters. External measurements indicate the time offsets between individual transmitters and UTC(USNO), and are currently available from four independent sources: VLF phase monitored at USNO, satellite/TV, Loran-C, and portable clock. Non-VLF measurements provide significantly increased accuracy over conventional VLF techniques, but are not currently available on a regular basis for all OMEGA transmitters.

This paper describes an integrated dynamic synchronization process currently implemented as Computer Program SYNC2. The program employs a linear data-mixing filter that appropriately combines mathematical models of cesium clock error dynamics with VLF and non-VLF timing measurements to estimate and control transmitter radiated phase and phase-rate offsets. The data-mixing filter has the inherent capability of optimizing OMEGA synchronization by making the best possible use of all available information including quantitative statistical descriptions of: cesium clock frequency uncertainties, timing measurement uncertainties, and measurement error time correlations. The discussion includes: cesium clock error modeling, measurement preprocessing, data-mixing filter formulation, synchronization adjustments, program input and output, and future plans for OMEGA synchronization.

Program SYNC2 is currently run each week by the U.S. Coast Guard OMEGA Navigation System Operations Detail, and is used to control OMEGA system synchronization to an accuracy on the order of 1 μ sec rms. A block diagram of the overall synchronization process is shown in Fig. 1.

R-22225

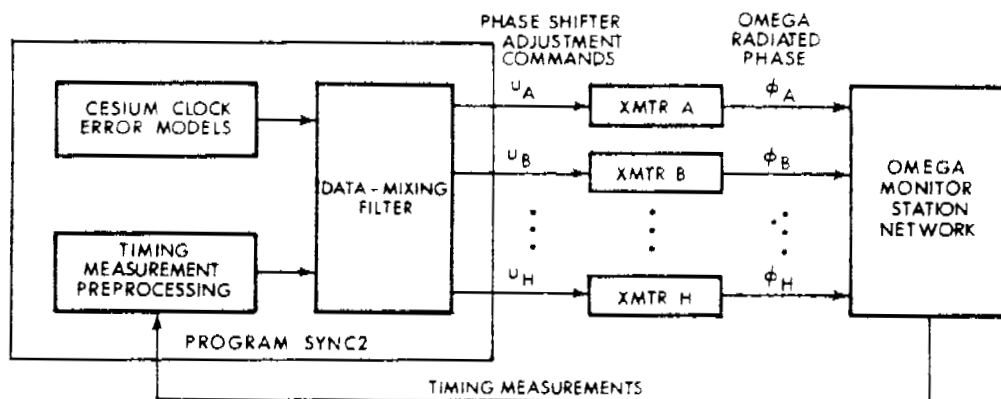


Fig. 1 — Integrated Synchronization Process

CESIUM CLOCK ERROR DYNAMICS

Program SYNC2 employs cesium clock error models to extrapolate transmitter synchronization offsets (both phase and phase rate) between times when synchronization measurements are available. Ignoring, for a moment, any phase shifter adjustments, the phase or time offset in μsec of transmitter I ($I = A, B, \dots, H$) relative to Mean OMEGA System Time can be represented by a standard cesium clock error model [4] at time t_{n+1} , i.e.,

$$[\delta\phi_{I\Omega}]_{n+1} = [\delta\phi_{I\Omega}]_n + \Delta T [\delta f_{I\Omega}]_n + [w_{I\Omega}^\phi]_n \quad (1)$$

and the phase rate (cesium frequency) offset in $\mu\text{sec/day}$ relative to Mean OMEGA System Time is given by

$$[\delta f_{I\Omega}]_{n+1} = [\delta f_{I\Omega}]_n + [w_{I\Omega}^f]_n \quad (2)$$

where

$w_{I\Omega}^\phi$ = zero-mean, white gaussian sequence corrupting the phase offset $\delta\phi$ caused by uncorrelated fluctuations in clock cesium frequency (phase rate)

$w_{I\Omega}^f$ = zero-mean, white gaussian sequence corrupting the phase rate δf caused by uncorrelated fluctuations in clock cesium frequency rate (phase acceleration)

ΔT = computation interval (0.5 day)

Random fluctuations in clock cesium frequency result in a random walk phase offset that grows proportional to the square root of time. The white sequence $w_{I\Omega}^\phi$, representing this effect in (1), is typically on the order of 0.019 μsec rms [4].

The white sequence $w_{I\Omega}^f$ in (2) produces a random walk frequency offset, and is used to approximate long-term random jumps in nominal cesium frequency as observed in empirical clock data [5] and [6]. Each discrete jump in cesium frequency, of magnitude $\Delta\delta f$ occurring after an N-day interval,

is approximated by a series of small jumps of magnitude $\Delta\delta f/2N$ occurring twice each day. The rms value of $w_{f\Omega}^f$ appropriate for this approximation, is given by

$$\sigma_{wf} = \Delta\delta f(2N)^{-\frac{1}{2}} \quad (3)$$

For a typical frequency jump magnitude of 0.03 μ sec/day and a typical interval between jumps of 15 days, (3) yields a σ_{wf} of 0.0055 μ sec/day. Since there is a lower bound on the uncertainty in an estimate of a random walk process [7], employing the white sequence $w_{f\Omega}^f$ in the clock model effectively prevents the data-mixing filter from becoming overly-confident in the accuracy of its cesium frequency estimate. Consequently, the filter is more responsive to any sudden change in the synchronization measurement trend brought about by a cesium frequency jump.

MEASUREMENT PREPROCESSING

The basic internal synchronization measurement involves a pair* of transmitters each with an associated monitor station. The associated monitor pair measures the VLF phase delay in each direction along the "reciprocal propagation path" between the transmitters as illustrated in Fig. 2. The monitors are close to, but not collocated with, their respective transmitters. Signals received at each monitor from the two transmitters are used to generate phase difference measurements. At monitor j, which receives signals from transmitters I and J, the phase difference measurement (I-J) is given by

$$\Delta\phi_{IJ}^j = \phi_{Ij} - \phi_{Jj} + \varepsilon_j \quad (4)$$

where

ϕ_{Ij} = phase of transmitter I received at monitor j

ϕ_{Jj} = phase of transmitter J received at monitor j

ε_j = instrumentation error at monitor j

*There are 28 possible transmitter pairs in an eight-transmitter system.



Fig. 2 — Typical Reciprocal Propagation Path

Compensation for Propagation Anomalies — The $\Delta\phi_{IJ}^j$ in (4) are corrected for propagation variations using a PPC value, and compared to a nominal phase difference (proportional to geodesic path length to the transmitters) to obtain an observed synchronization offset between transmitters I and J:

$$\text{OBS}_{IJ}^j = \Delta\phi_{IJ}^j + \text{PPC}_{IJ}^j - \text{NOM}_{IJ}^j \quad (5)$$

The quantity OBS_{IJ}^j in (5) is called an "observed" offset because it includes not only the actual synchronization offset between I and J, but also instrumentation errors and residual propagation errors (i.e., errors due to unpredicted propagation variations). PPC errors are typically the dominant error source with magnitudes on the order of 3 to 12 μsec .

Reciprocal Path Phase Differencing — A significant portion of the PPC error in (5) is independent of direction along the path (i.e., the PPC error for propagation from transmitter I to monitor j is approximately equal to the PPC error for propagation from transmitter J to monitor i). This fact can be used to advantage by differencing the two observed synchronization offsets measured in each direction to yield

$$z_{IJ} = \frac{1}{2} (\text{OBS}_{IJ}^j - \text{OBS}_{JI}^i) \quad (6)$$

Direction-independent PPC errors (e.g., solar illumination and ground conductivity) tend to cancel out in (6)*. The

*This technique was originally developed in [8].

quantity z_{IJ} is a relative synchronization offset measurement for transmitters I and J. It is shown in [9] that z_{IJ} is of the form

$$z_{IJ} = \delta\phi_{IJ} + v_{IJ} \quad (7)$$

where $\delta\phi_{IJ}$ is the actual phase (or time) offset between transmitters I and J, and v_{IJ} is a measurement error, typically on the order of 1.0 - 2.5 μ sec rms, which includes only direction-dependent PPC errors and uncorrelated instrumentation errors.

Outlier Rejection - Program SYNC2 includes a comprehensive algorithm designed to detect and reject VLF measurement outliers as described in Appendix A.

Measurement-Quality Weighting - SYNC2 includes a special routine to estimate VLF measurement errors for use in specifying measurement quality in the data-mixing filter. Each VLF measurement error is approximated by the rms "fit error" between actual synchronization measurements and those predicted by SYNC2 models over each previous three-week period. Specifically, the measurement fit error at time t_n is defined as*

$$[\delta z_{IJ}]_n = [z_{IJ}]_n - [\hat{z}_{IJ}]_n \quad (8)$$

where the predicted measurement is

$$[\hat{z}_{IJ}]_n = [\hat{\delta\phi}_{I\Omega}]_n - [\hat{\delta\phi}_{J\Omega}]_n \quad (9)$$

and $\hat{\delta\phi}_{I\Omega}$ is the filter estimate of the internal phase (or time) offset of transmitter I relative to Mean OMEGA System Time. SYNC2 computes the rms fit error over the three-week period prior to each daily measurement, and repeatedly updates this statistic after each daily measurement is processed. The mean square fit error is used to define a measurement noise covariance matrix R_n which accounts for measurement quality in the data-mixing filter.

*The overhat (^) denotes an estimated parameter.

Time-Correlation Modeling - VLF measurement errors are generally correlated in time due to residual diurnal (daily) and seasonal propagation variations not removed by published PPCs. Analysis of empirical data [10] indicates that the normalized autocorrelation function of the daily measurement errors v_{IJ} in (7) can be approximated by an exponential function of the form*

$$R_v(\tau) = E \left\{ v(t) v(t+\tau) \right\} / E \left\{ v^2(t) \right\} \approx \exp(-|\tau|/\tau_o) \quad (10)$$

where τ is time shift in days, and τ_o is determined from empirical data. (A "best fit" is obtained for $\tau_o \approx 2.5$ days.) From (10), the daily measurement error is modeled as a first-order markov process:

$$\begin{bmatrix} v_{IJ} \end{bmatrix}_{n+2} = \exp(-2\Delta T/\tau_o) \begin{bmatrix} v_{IJ} \end{bmatrix}_n + \begin{bmatrix} \eta_{IJ} \end{bmatrix}_n \quad (11)$$

where $\Delta T = 0.5$ day is the computation interval, and η_{IJ} is a zero-mean, white, gaussian sequence representing the uncorrelated components of v_{IJ} . The variance of v_{IJ} is denoted by σ_{IJ}^2 , and is approximated by the mean square value of the measurement fit error over each previous three-week period. The corresponding variance of η_{IJ} is computed as [7].

$$\begin{bmatrix} \sigma_{IJ}^2 \end{bmatrix}_n = \begin{bmatrix} \sigma_{IJ}^2 \end{bmatrix}_n \{ 1 - \exp(-4\Delta T/\tau_o) \} \quad (12)$$

EXTERNAL TIMING MEASUREMENTS

External timing measurements for synchronization to UTC(USNO) are currently available for four of eight OMEGA transmitters. OMSTAs Liberia, Trinidad and North Dakota are linked to UTC by one-way VLF phase measurements; OMSTA Hawaii has been linked via satellite/TV, Loran-C, and several portable clock visits each year [11]. A Loran-C timing link between OMSTA North Dakota and UTC is planned for the near future.

*The symbol $E\{\cdot\}$ denotes expected (or ensemble average) value.

An external synchronization measurement of UTC relative to transmitter I ($I = A, B, \dots, H$) is expressed in the form

$$z_{RI} = \delta\phi_{RI} + v_{RI} \quad (13)$$

where $\delta\phi_{RI}$ is the actual external phase (or time) offset of transmitter I, and v_{RI} is the measurement error. For filter mechanization, (13) is expressed in an equivalent form in terms of the internal phase offset $\delta\phi_{I\Omega}$ of transmitter I (relative to Mean OMEGA System Time) and the external offset $\delta\phi_{R\Omega}$ of UTC relative to Mean OMEGA System Time, i.e.,

$$z_{RI} = \delta\phi_{R\Omega} - \delta\phi_{I\Omega} + v_{RI} \quad (14)$$

Internal and external measurement errors, as modeled in the data-mixing filter are summarized in Table 1. External VLF phase measurements are generally not as accurate as internal VLF measurements since the reciprocal path differencing technique in (6) cannot be employed for one-way propagation. However, external VLF bias errors are dynamically calibrated and removed by comparing them to more-accurate non-VLF measurements when available. Non-VLF measurement errors are discussed in detail in [11].

TABLE 1 SYNCHRONIZATION MEASUREMENT ERRORS

Synchronization Measurement Type	RMS Error (usec)
Internal VLF phase	1.0 - 2.5*
External VLF phase	1.1 - 2.6*
Loran-C	0.21 or 0.28†
Satellite/TV	0.11 or 0.21†
Portable clock	0.07 or 0.19†

*Typical values dynamically computed for each daily measurement based on 3-week rms fit error as defined in (8).

†Accuracies reflect dynamic and static calibration, respectively, of the phase advance between each transmitter's radiated signal and its online cesium clock.

ESTIMATION ALGORITHM

System State Equation - The clock error dynamics model in (1) and (2) is expressed in a vector-matrix system state equation for all eight OMEGA transmitters (A, B, ..., H) at time t_n as

$$\begin{bmatrix} \delta\phi_{A\Omega} \\ \delta\phi_{B\Omega} \\ \vdots \\ \vdots \\ \delta\phi_{H\Omega} \\ \delta\phi_{R\Omega} \\ \delta f_{A\Omega} \\ \delta f_{B\Omega} \\ \vdots \\ \vdots \\ \delta f_{H\Omega} \\ \delta f_{R\Omega} \end{bmatrix}_{n+1} = \begin{bmatrix} 1 & 0 & \Delta T & 0 & \\ 0 & 1 & \Delta T & 0 & \\ \vdots & \vdots & \ddots & \ddots & 0 \\ 0 & 0 & 0 & \Delta T & \\ 0 & 1 & 0 & 0 & \Delta T \\ 0 & 0 & 1 & 0 & \\ 0 & 0 & 0 & \ddots & 0 \\ 0 & 1 & 0 & 0 & 1 \end{bmatrix} \cdot \begin{bmatrix} \delta\phi_{A\Omega} \\ \delta\phi_{B\Omega} \\ \vdots \\ \vdots \\ \delta\phi_{H\Omega} \\ \delta\phi_{R\Omega} \\ \delta f_{A\Omega} \\ \delta f_{B\Omega} \\ \vdots \\ \vdots \\ \delta f_{H\Omega} \\ \delta f_{R\Omega} \end{bmatrix}_n + \begin{bmatrix} w_{A\Omega}^\phi \\ w_{B\Omega}^\phi \\ \vdots \\ \vdots \\ w_{H\Omega}^\phi \\ w_{R\Omega}^\phi \\ w_{A\Omega}^f \\ w_{B\Omega}^f \\ \vdots \\ \vdots \\ w_{H\Omega}^f \\ w_{R\Omega}^f \end{bmatrix}_n + \begin{bmatrix} u_A \\ u_B \\ \vdots \\ \vdots \\ u_H \\ 0 \\ 0 \\ 0 \\ \vdots \\ \vdots \\ 0 \\ 0 \end{bmatrix}_n \quad (15)$$

or, more compactly*

$$\underline{x}_{n+1} = \underline{\Phi}\underline{x}_n + \underline{w}_n + \underline{u}_n \quad (16)$$

where $\underline{\Phi}$ is the state transition matrix, and the control vector \underline{u}_n accounts for phase shifter adjustments applied to each clock during the computation interval ΔT . The elements $\delta\phi_{R\Omega}$ and $\delta f_{R\Omega}$ represent the external phase and frequency offsets, respectively, of UTC relative to Mean OMEGA System Time.

Measurement Equation - The internal synchronization measurements in (7), and the external measurements in (14) are combined as

*A bar beneath a symbol denotes a vector.

$$\begin{array}{c|c|c|c|c|c|c}
 z_{AB} & 1 & -1 & & & & \delta\phi_{A\Omega} & v_{AB} \\
 z_{AC} & & 1 & 0 & -1 & 0 & \delta\phi_{B\Omega} & v_{AC} \\
 \cdot & & & \cdot & \cdot & 0 & \cdot & \cdot \\
 \cdot & & & & \cdot & 0 & \cdot & \cdot \\
 z_{AH} & = & 1 & 0 & \cdots & 0 & -1 & \frac{\delta\phi_{H\Omega}}{n} + v_{AH} \\
 z_{BC} & & 0 & 1 & -1 & & & v_{BC} \\
 z_{BD} & & 0 & 1 & 0 & -1 & & v_{BD} \\
 \cdot & & \cdot & \cdot & \cdot & 0 & 0 & \cdot \\
 \cdot & & \cdot & \cdot & \cdot & & 0 & \cdot \\
 z_{BH} & & 0 & 1 & 0 & \cdots & 0 & -1 & v_{BH} \\
 \cdot & & & & \cdot & & & \cdot \\
 \cdot & & & & \cdot & 0 & 0 & 0 & v_{GH} \\
 \cdot & & & & \cdot & & 0 & 0 & 0 \\
 z_{GH} & & 0 & \cdot & \cdot & 0 & 1 & -1 & 0 \\
 0 & & 1 & 1 & \cdots & 1 & 0 & 0 & 0 \\
 z_{RA} & & -1 & & & & 1 & & v_{RA} \\
 z_{RB} & & -1 & & 0 & & 1 & & v_{RB} \\
 \cdot & & \cdot & & \cdot & & \cdot & & \cdot \\
 \cdot & & 0 & & \cdot & & \cdot & & \cdot \\
 z_{RH} & & & & & -1 & 1 & & v_{RH} \\
 \end{array}$$

(17)

or, more compactly as

$$\underline{z}_n + H_n \underline{x}_n + \underline{v}_n \quad (18)$$

The measurement matrix H_n has 18 columns and up to 37 rows, depending on measurement availability (typically, 16 are available). If any measurement is not available at a particular sample time, the corresponding rows are deleted from (17).

Measurement Constraint - The zero element in the measurement vector \underline{z}_n in (17) represents an internal "measurement constraint" which is included for convenience to avoid a singular measurement matrix. In general, for an N-transmitter system, there are $N(N-1)/2$ different reciprocal paths (see Fig. 2), but only $N-1$ paths provide independent measurements. This can cause computational difficulty in attempting to determine eight transmitter timing offsets from only seven independent measurements. One approach to this problem is to arbitrarily define the mean internal timing offset (Mean OMEGA System Time) as zero, i.e.,

$$\phi_{\Omega} = \frac{1}{8} \sum_{I=A}^H \delta\phi_{I\Omega} \equiv 0 \quad (19)$$

Then, it is possible to define, as an internal measurement constraint, an "error-free" measurement of Mean OMEGA System Time as

$$z_{\Omega} = \frac{1}{8} \sum_{I=A}^H \delta\phi_{I\Omega} \equiv 0 \quad (20)$$

The measurement constraint in (20), used in conjunction with seven independent measurements, allows a direct computation* of eight internal timing offsets.

For the complete eight-transmitter system (with 28 possible reciprocal paths), internal synchronization offsets can theoretically be determined using relative phase measurements from any seven independent paths. In the absence of measurement and propagation prediction errors, the estimation error using any seven independent paths would be zero. However, since there are always residual measurement and modeling errors, it is desirable to use redundant data from as many paths as possible to minimize the effects of these errors on system synchronization.

A Priori Information - Implementation of the data-mixing filter requires a priori information on: clock cesium frequency disturbances w_n in (16), synchronization measurement errors v_n in (18), initial state estimate $\hat{\underline{x}}_0$, and initial state estimation error \underline{x}_0 , i.e.,

*Alternative techniques involve the use of a "pseudo-inverse" matrix and produce identical results.

$$\tilde{\underline{x}}_0 = \hat{\underline{x}}_0 - \underline{x}_0 \quad (21)$$

Typically, the initial state estimates for the current week are set equal to the final estimates from the previous week. (For an unsynchronized transmitter, the initial estimates are set to zero.) The remaining parameters, \underline{w}_n , \underline{v}_n and $\tilde{\underline{x}}_0$, are described statistically in terms of the diagonal covariance matrices:

$$Q = E\left\{\underline{w}_n \underline{w}_n^T\right\} \quad (22)$$

$$R_n = E\left\{\underline{v}_n \underline{v}_n^T\right\} \quad (23)$$

$$P_0 = E\left\{\tilde{\underline{x}}_0 \tilde{\underline{x}}_0^T\right\} \quad (24)$$

The elements of Q , R_n and P_0 are given in Table 2.

TABLE 2 A PRIORI STATISTICS

Covariance Matrix	Diagonal Element	Value	Units
Q	$\sigma_{w\phi}^2$	3.6×10^{-4}	μsec^2
	σ_{wf}^2	0.3×10^{-4}	$(\mu\text{sec}/\text{day})^2$
R_n	$[\sigma_{IJ}]_n^2$	See Table 1	μsec^2
P_0	$[\sigma_{I\Omega}^\phi]_0^2$	Final values from previous week*	μsec^2
	$[\sigma_{I\Omega}^f]_0^2$	↓	$(\mu\text{sec}/\text{day})^2$

*For an unsynchronized transmitter, typical values are $100 \mu\text{sec}^2$ phase uncertainty and $0.75 (\mu\text{sec}/\text{day})^2$ frequency uncertainty.

Data-Mixing Filter - A linear dynamic estimation algorithm for computing OMEGA synchronization offsets can be formulated in terms of the basic system model defined in (16) and (18). The resulting formulation is referred to as a Kalman (data-mixing) filter [7] and is summarized in Fig. 3. The diagonal elements of the covariance matrix P_n in Fig. 3 provide an indication of the uncertainty associated with each synchronization estimate \hat{x}_n . Implementation of these equations in Program SYNC2 is discussed in detail in [12].

Measurement Correlation - A necessary condition for implementation of the data-mixing filter in Fig. 3 is that the measurement errors v_n in (18) are uncorrelated in time (i.e., a white sequence). However, VLF measurement errors are, in fact, time-correlated. This problem is circumvented by employing a measurement-differencing technique as outlined in [13]. This technique produces differenced measurement errors that are uncorrelated in time, and allows the resulting system model to be written in a form equivalent to that defined in (16) and (18).

OPTIMAL ESTIMATE

$$\hat{x}_n^- = \Phi \hat{x}_{n-1}^+ + u_{n-1} \quad \text{EXTRAPOLATION BETWEEN MEASUREMENTS} \quad (25)$$

$$\hat{x}_n^+ = \hat{x}_n^- + K_n [z_n - H_n \hat{x}_n^-] \quad \text{MEASUREMENT UPDATE} \quad (26)$$

$$K_n = P_n^- H_n^T [H_n P_n^- H_n^T + R_n]^{-1} \quad \text{WEIGHTING} \quad (27)$$

ESTIMATION ERROR COVARIANCE

$$P_n^- = \Phi P_{n-1}^+ \Phi^T + Q \quad \text{EXTRAPOLATION BETWEEN MEASUREMENTS} \quad (28)$$

$$P_n^+ = [I - K_n H_n] P_n^- \quad \text{MEASUREMENT UPDATE} \quad (29)$$

Fig. 3 — Data-Mixing Filter Formulation

SYNCHRONIZATION ADJUSTMENTS

OMEGA synchronization control is physically implemented by periodically adjusting the phase shifter of each transmitter's online cesium clock. Two types of adjustments are applied: a weekly adjustment to correct for the phase (or time) offset existing at the beginning of each week, and a four-hour adjustment (i.e., applied every four hours) to correct for expected phase drift (due to cesium frequency offset) during the week.

The synchronization control task is complicated by communications delays between the eight transmitter/monitor stations and the OMEGA Data Processing Center in Washington, D.C. Additional delays are introduced in data processing, resulting in a time lag of 40 hours between the last synchronization measurements taken each week and the application of new weekly and four-hour adjustments. This lag can be significant if the computed four-hour adjustment command for a particular cesium clock changes significantly from one week to the next. A special adjustment is made to compensate for this effect as discussed below.

The weekly adjustment for transmitter I($I = A, B, \dots, H$) consists of two basic components: an estimated external phase offset (UTC-transmitter I) based on the latest available measurements, and special compensation (if necessary) for ten obsolete four-hour adjustments applied during the 40 hour lag discussed above. The four-hour adjustment for transmitter I is simply the external frequency offset estimate (UTC-transmitter I) in $\mu\text{sec}/4\text{-hr}$.

SAMPLE OUTPUT

A typical time history of internal synchronization measurements print-plotted by Program SYNC2 is shown in Fig. 4. Both 10.2 and 13.6 kHz reciprocal-path phase-difference measurements of transmitter pair DG (north Dakota minus Trinidad) are given for the period from 24 November 1975 to 5 January 1976. SYNC2 adjustment commands were used to control system synchronization throughout this period. The last three weeks of measurements in Fig. 4 have a standard deviation on the order of 1 usec and mean value on the order of -1 usec. This -1 usec bias represents either a measurement bias error, an actual phase offset between transmitters D and G, or some combination of both. SYNC2 employs the measurement fit error computation in (8) to account for measurement bias errors (which, in this case, were -0.4 usec).

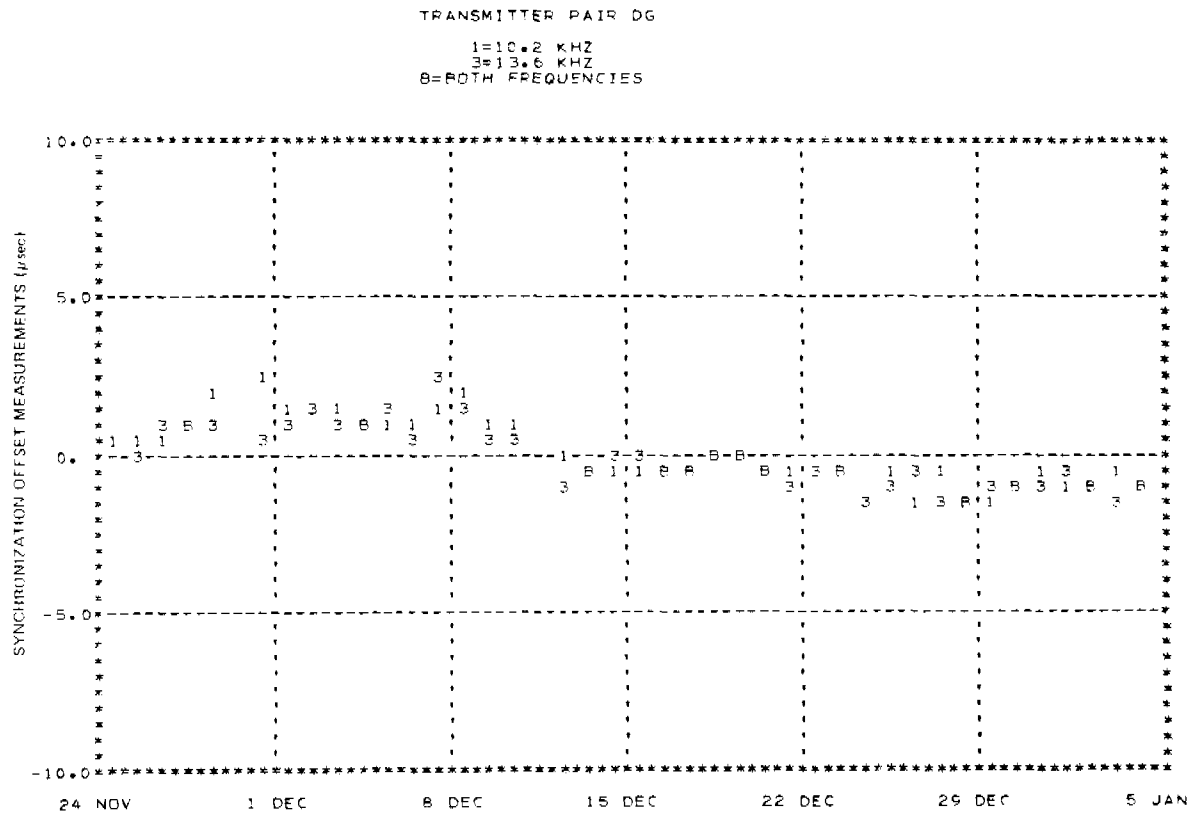


Fig. 4 — Synchronization Measurements (North Dakota Minus Trinidad)

A time history plot of synchronization offset estimates (both phase and cesium frequency) computed for OMSTA North Dakota (transmitter D) is shown in Fig. 5. Estimates immediately after each twice-daily measurement update are shown for the same six-week period indicated in Fig. 4. The abrupt change in the phase offset estimate from (-0.5 to 0.0 μ sec) on 26 November reflects a weekly phase shifter adjustment. The abrupt change in the frequency offset estimate (from 0.08 to -0.6 μ sec/day) on 15 December reflects a replacement of the online clock for transmitter D by one of its backup clocks. (Frequency offset estimates for backup clocks are computed in a separate algorithm by least-squares fit to online clock data.)

The rms uncertainties for the estimates in Fig. 5 are derived from (28) and (29) and are plotted in Fig. 6. SYNC2 automatically increases the frequency offset uncertainty to 0.2 μ sec whenever an online clock is replaced, as shown in Fig. 6. In general, as more measurements are processed, estimate uncertainties (both phase and cesium frequency)

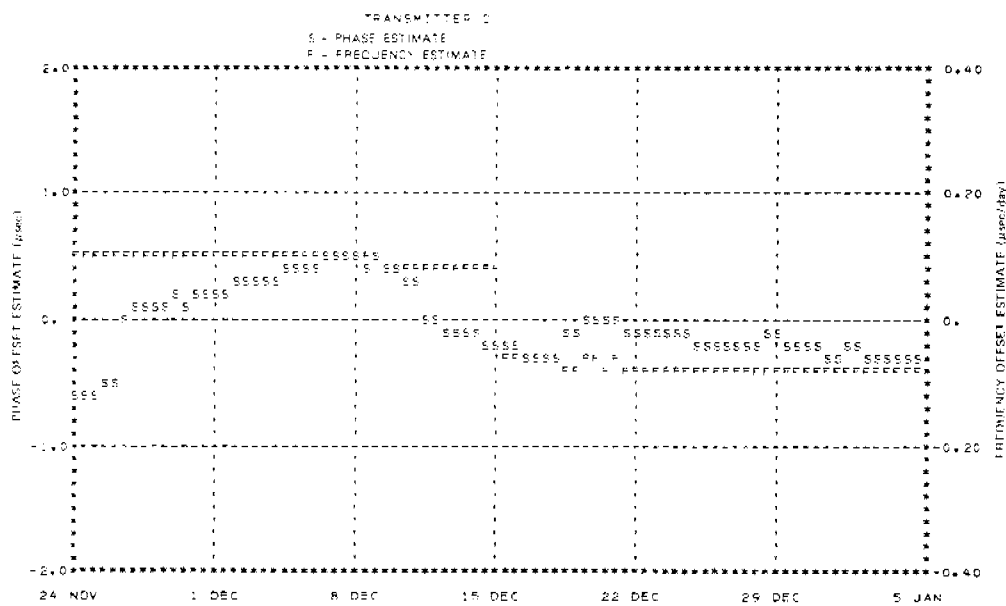


Fig. 5 — Synchronization Estimates

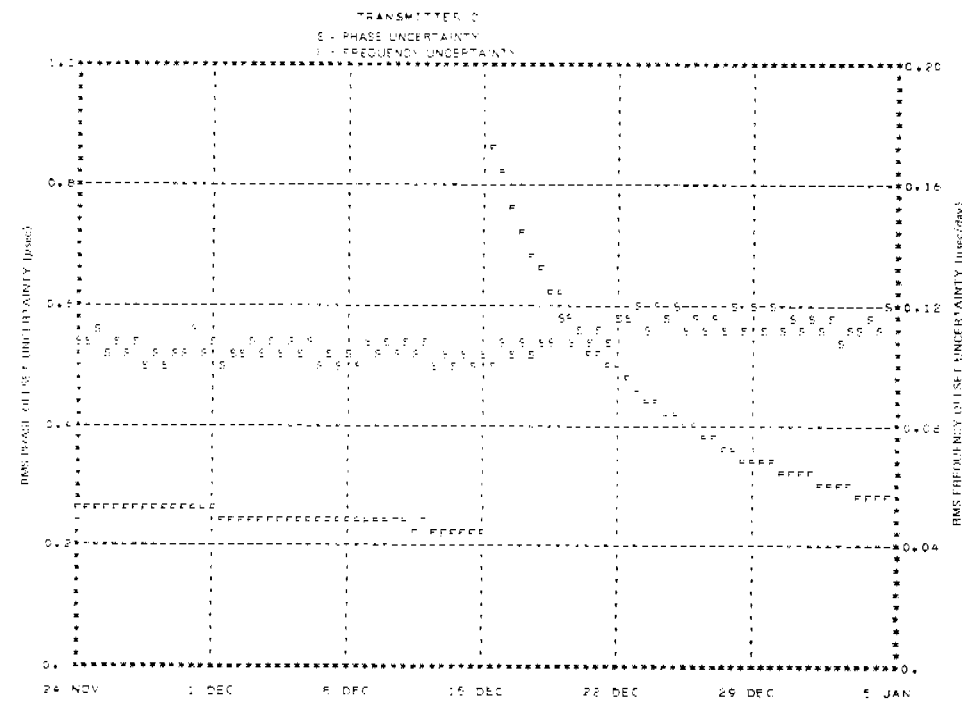


Fig. 6 — Estimate Uncertainties

decay exponentially to non-zero steady-state values. (The slight increase in phase uncertainty after 15 December, results from the large frequency offset uncertainty for the new online clock.) The exponential decay rates depend on: measurement accuracy, measurement interval, and measurement error correlation. The steady-state values depend on measurement accuracy and random fluctuations in clock cesium frequency and frequency rate.

Figures 5 and 6 indicate that on 5 January 1976 the internal phase offset for transmitter D was -0.3 ± 0.6 μ sec relative to Mean OMEGA System Time, and the transmitter online clock had a natural phase drift rate (frequency offset) of -0.08 ± 0.06 μ sec/day relative to Mean OMEGA System Time. Based on these estimates, the internal weekly adjustment was on the order of 0.3 μ sec, and the four-hour adjustments for the subsequent week were 0.01 μ sec.

A time history plot of external measurements (UTC minus Hawaii) via Loran-C timing links is shown in Fig. 7. These measurements indicate that OMSTA Hawaii was synchronized to UTC within an accuracy on the order of 1 μ sec for the period 13 September to 25 October 1976. External non-VLF measurements (when available) provide an excellent means of checking (as well as maintaining) synchronization accuracy of the OMEGA system.

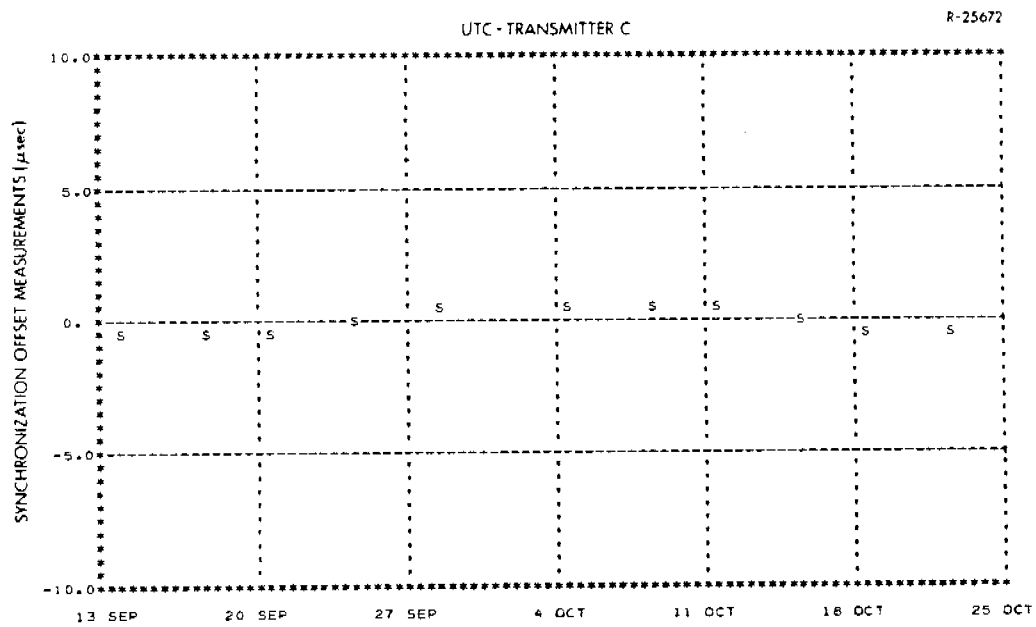


Fig. 7 -- Loran-C Measurements (UTC Minus Hawaii)

FUTURE PLANS

Timing Measurements - Reciprocal VLF timing measurements in (7) are generally accurate to a few μ sec when direction-dependent propagation prediction errors are small. Operational experience has revealed two situations where these errors are, in fact, significant: near the magnetic equator and near the geographic poles. Recent portable clock measurements [14] and [15] indicate propagation anomalies on the order of 3-9 μ sec in some VLF measurements for OMSTA Reunion (which is south of the magnetic equator). Polar-path synchronization measurements involving OMSTA Norway are significantly degraded in the spring and fall due to changing solar illumination conditions. In order to minimize adverse effects of the above phenomena, future efforts related to OMEGA synchronization accuracy will most likely follow two basic avenues: accuracy improvement via refinement of existing VLF propagation prediction models [2], and accuracy verification (and improvement) via increased use of non-VLF timing links such as satellite/TV, Loran-C, and portable clock measurements.

Leap Second Offset - Mean OMEGA System Time currently leads UTC(USNO) by five seconds. Although operational procedures do exist for inserting leap second timing adjustments at each OMEGA transmitter, there are currently no plans to eliminate this offset from UTC. OMEGA leap second offset information is announced in ONSOD's Weekly Status Message and on WWV.

JMSA Participation - At the September 1976 OMEGA Technical Conference in Bergen, Norway, OMEGA Member nations supported a resolution to transfer OMEGA synchronization operations from ONSOD to the Japanese Maritime Safety Agency (JMSA). JMSA has completed test runs of Program SYNC2 and is currently maintaining data files in parallel with ONSOD on a weekly basis. After official transfer of Program SYNC2 operations to JMSA, ONSOD will maintain parallel data files to ensure a smooth transition. In order to maintain system synchronization to UTC(USNO), JMSA will continue to use UNSO data as the primary source of external timing measurements.

SUMMARY

This paper describes the application of modern estimation techniques to the problem of synchronizing the OMEGA radio navigation system to an accuracy on the order of 1 μ sec rms.

In order to achieve this accuracy, extensive preprocessing is performed on VLF timing measurements to reduce the effects of VLF propagation anomalies. The noisy, time-correlated VLF measurements are then processed in a Kalman data-mixing filter that appropriately combines them with cesium clock error models to estimate OMEGA transmitter timing offsets and compute timing adjustment commands. The synchronization algorithm is mechanized in Computer Program SYNC2 which was developed by The Analytic Sciences Corporation and implemented in January 1975. Program SYNC2 is run each week by the U.S. Coast Guard OMEGA Navigation System Operations Detail to control both internal and external system synchronization.

APPENDIX A VLF OUTLIER REJECTION

SYNC2 employs an automatic outlier rejection scheme to identify and remove VLF measurements that are not "statistically representative" of the total data set. It is assumed that, on the average, 95% of the measurements are statistically representative and 5% are outliers. Prior to applying an outlier rejection test, two distorting effects are removed from the measurements: the effect of weekly phase shifter adjustments, and any nonzero trend over the previous six weeks. The resulting data set is assumed to be normally (gaussian) distributed about the trend line.

For normally distributed data, 95% of the measurements lie within 1.96 standard deviations (1.96σ) of the trend line [16]. Typically, the true σ of the data set can only be approximated by a sample standard deviation $\hat{\sigma}$, and this approximation is good only for large data samples (i.e., 30 or more measurements). Frequently, however, due to transmitter outages, monitor outages, or previously rejected data, there may be significantly less than 30 daily VLF measurements available for a particular transmitter-pair in a given six-week period.

A more appropriate rejection criterion for this situation is developed in [16] and [17] where it is shown that for n normally distributed measurements, 95% lie within $k\hat{\sigma}$ of the trend line, where

$$k = \frac{T \sqrt{n - 1}}{\sqrt{n - 2 + T^2}}, \quad n \geq 3 \quad (33)$$

and T is the value of the Student's probability distribution function for 0.05 level of significance and n-2 degrees of freedom. As the number of daily measurements increases from 3 to a maximum of 42, k increases from 1.41 to 1.95 ($k = 1.96$ for $n \rightarrow \infty$).

SYNC2 employs an iterative \hat{k} outlier rejection scheme that: computes a six-week sample standard deviation $\hat{\sigma}$ about the measurement trend line, rejects all measurements exceeding $\hat{k}\hat{\sigma}$ from the trend line, and repeats this process until no new outliers are found.

REFERENCES

1. Swanson, E.R., and Brown, R.P., "OMEGA Propagation Prediction Primer," Naval Electronics Laboratory Center, Technical Note TN-2101, August 1972.
2. United States Coast Guard OMEGA Navigation System Operations Detail, "OMEGA Propagation Prediction Model and Computer Program Documentation," April 1973.
3. Defense Mapping Agency Hydrographic Center (DMAHC), "OMEGA Propagation Correction Tables," H.C. Publication Series No. 224.
4. Autonetics Div., North American Rockwell Corp., "Analysis of Advanced Time-Frequency National Air Space System Concept, Volume II, Time and Frequency Techniques Survey," Report No. RD-69-32, August 1969.
5. Hafele, J.C., "Performance and Results of Portable Clocks in Aircraft," Proceedings of the Third Annual PTTI Planning Meeting, November 1971.
6. Winkler, G.M.R., et.al., "The USNO Clock Time Reference, and Performance of a Sample of Atomic Clocks," Metrologia, Vol. 6, 1970.
7. Gelb, A., Ed., Applied Optimal Estimation, M.I.T. Press, Cambridge, 1974.
8. Pierce, J.A., et.al., "OMEGA: A Worldwide Navigational System, System Specification and Implementation, Second Revision," Office of Naval Research, DDC No. AD-630-900, May 1966.

9. Swanson, E.R., and Kugel, C.P., "VLF Timing-Conventional and Modern Techniques," Proceedings of the IEEE, Vol. 60, No. 5, May 1972.
10. D'Appolito, J.A., and Kasper, J.F., "Predicted Performance of an Integrated OMEGA/Inertial Navigation System," National Aerospace Electronics Conference, Dayton, Ohio, May 1971.
11. Lavanceau, J.D., "OMEGA Signals and Universal Time," First OMEGA Symposium, Tokyo, Japan, June 1975.
12. Schane, R.N., "Linear Dynamic Estimation and Control of OMEGA Radio Navigation System Synchronization," Proceedings of the 1976 IEEE Conference on Decision and Control, Clearwater Beach, Florida, December 1976.
13. Bryson, A.E., and Henrikson, L.J., "Estimation Using Sampled Data Containing Sequentially Correlated Noise," Journal of Spacecraft and Rockets, Vol. 5, No. 6, June 1968.
14. Fisher, L.C., United States Naval Observatory, Personal Communication, 19 July 1976.
15. Vannicola, V., United States Coast Guard OMEGA Navigation System Operations Detail, Personal Communication, 20 July 1976.
16. Cramer, H., Mathematical Methods of Statistics, Princeton University Press, 1974.
17. Swaroop, R., and West, K.A., "A Simple Technique for Automatic Computer Editing of Biodata," National Aeronautics and Space Administration, Technical Note NASA-TN-D-5275, June 1969.

ACKNOWLEDGEMENTS

The authors acknowledge the encouragement provided throughout this effort by Mr. David C. Scull of ONSOD, and the helpful suggestions of Drs. John E. Bortz and Joseph F. Kasper of TASC during algorithm development.